Effects of substrate temperature and ion current density on the structure of silicon-on-insulator material implanted with low-energy oxygen

1993 J. Phys.: Condens. Matter 5 1291

(http://iopscience.iop.org/0953-8984/5/9/013)

J. Phys.: Condens. Matter 5 (1993) 1291–1298. Printed in the UK

Effects of substrate temperature and ion current density on the structure of silicon-on-insulator material implanted with low-energy oxygen

Yukari Ishikawa and Noriyoshi Shibata
Japan Fine Ceramics Centre, 2-4-1 Mutsuno, Atsuta-ku, Nagoya, 456 Japan

Received 26 October 1992, in final form 1 December 1992

Abstract. Thin silicon-on-insulator (SOI) film formation during 25 keV O^+ ion implantation has been investigated by cross-sectional transmission electron microscopy, Auger electron spectroscopy and scanning electron microscopy. The top Si layer thickness in as-implanted samples increased with increasing substrate temperature from 280 to about 500 °C and the current density from 10 to 450 μA cm^{-2} at a constant dose of 2×10^{17} ion cm^{-2}. Substrate heated to about 485 °C showed remarkable *in situ* annealing effects during ion implantation; resulting in the oxygen depth profile and the increase of the Si–O bonding. The SOI structure was formed in a wide range of the current density at about 485 °C. Shallow holes appearing in the surface at substrate temperatures higher than 485 °C scarcely influenced subsequent SOI structure formation. Deep holes appearing above 530 °C made it difficult to produce the SOI structure.

1. Introduction

Recently, thin silicon-on-insulator (SOI) films have become very attractive for future applications in ultra small metal-oxide–semiconductor field-effect-transistor (MOSFET) devices. Several studies have pointed out remarkable application advantages of the very thin SOI films [1–4] thinner than 100 nm compared with conventional thick SOI films: improvement of subthreshold characteristics [5], suppression of the kink effect [6, 7], reduction of the short-channel effect [8, 9] and increase in transconductance [10, 11]. Separation by implanted oxygen (SIMOX) is a leading process in producing the desired SOI structures [12]. We have reported in a previous paper [13] that SOI films can be formed by oxygen ion (O^+) implantation with an energy range as low as 15–30 keV. Low-energy oxygen ion implantation into silicon reduces the projected range of the ions and, therefore, forms a buried oxide layer close to the surface. The thicknesses of the top silicon layer and the buried oxide layer were 48 and 61 nm, respectively, for the Si wafer implanted with 25 keV O^+ with a dose of 2×10^{17} ion cm^{-2}. There are a few further reports on thin SOI film preparation by low-energy O^+ in the range of 50–140 keV [14] and 30–80 keV [15].

In low-energy SIMOX, the SOI structure obtained is very sensitive to the implantation conditions, because the top Si layer is far thinner than in the conventional SIMOX process using 150–200 keV ions. In addition, the silicon surface has far higher oxygen concentration due to the short projection range of the ions than conventional SIMOX. Also, the appropriate oxygen dose which forms the SOI structure is far smaller than the conventional SIMOX dose using 1–2 × 10^{18} ion cm^{-2}. Therefore, precise control of the implantation conditions based on an understanding of the SOI film-producing mechanism is essential in achieving device-grade SOI films.

In this paper, effects on the SOI structure of substrate temperature and current density during low-energy ion implantation have been investigated to clarify the mechanism of thin SOI film production. New results based on low-energy and low-dose implantation such as the *in situ* annealing effect have been observed. The results of the low-energy SIMOX process compared with conventional SIMOX [16, 17] are discussed.

2. Experimental procedure

The substrates used in this study were Sb-doped n-type Si (111) wafers 4° off toward ⟨011⟩ with a resistivity below 0.03 Ω cm. The Si (111) surface was expected to be suitable for ion implantation due to surface stability. Before the ion implantation, the substrates were cleaned by wet chemical and thermal processes. After the first degreasing process, the second acid treatment was carried out. The acid treatment involves boiling in a H_2SO_4–H_2O_2 2:1 solution bath to etch the Si surface region and to form the oxide layer, then dipping in a HF–H_2O 1:2 solution to remove the oxide layer. Finally, the thermal process was conducted in a vacuum just before implantation. The substrates were heated at about 850 °C for half an hour.

The ion implantation was carried out using an electron-cycrotron-resonance (ECR) bucket ion source (ULVAC MB62–5219) [18]. The ions were implanted at an energy of 25 keV. The O^+ ion current density was varied from 10 to 450 μA cm^{-2}. The ion current density was monitored by a Faraday cup in front of the substrate. The substrates were heated at temperatures from 280 to 710 °C. The substrate temperature was monitored by a thermocouple mounted on the heater behind the substrate, and also by a pyrometer (Minolta IR308). Substrate temperature change caused by the ion implantation was also measured by the pyrometer. Chamber pressure was held below 2×10^{-4} Pa. After ion implantation, the substrates were cooled without annealing.

Cross-sectional microstructures of Si wafers implanted with O^+ were investigated by using a transmission electron microscope (TEM) with a 350 keV beam (JEOL type JEM–4000FX). Specimens for the TEM observation were prepared by polishing and argon ion milling. Oxygen depth profiles were analysed by Auger electron spectroscopy (AES) (JEOL type JAMP 10SX). The depth profiling was accomplished by sputtering a 2 × 2 mm^2 area of the O^+ implanted sample surface using an Ar ion beam. The area analysed was 5 μm in diameter.

3. Results and discussion

3.1. Dependence of substrate temperature

3.1.1. SOI structure. Cross-sectional microstructures for Si implanted with 25 keV O^+ without high-temperature annealing are shown in figure 1. Substrate temperature measured just before the ion implantation was (*a*) 280 °C and (*b*) 485 °C. The substrate temperature increased and soon saturated during the ion implantation. Temperature increase caused by an ion current density of 450 μA cm^{-2} was about 60 °C and 20 °C for (*a*) and (*b*), respectively. Under the implantation conditions with the dose of

2×10^{17} ion cm^{-2} and the current density of 450 $\mu A\ cm^{-2}$, the SOI structures were formed at both substrate temperatures. However, the structures were different in the two cases. In the sample implanted at 280 °C, the top Si layer was thinner and the amorphous SiO_x layer thicker than the corresponding layers in the sample implanted at 485 °C. The interface between the Si layer and the amorphous SiO_x layer was very flat for the implantation at 280 °C, while the interface became uneven for the implantation at 485 °C. The thickness of the top Si layer increased and the thickness of the amorphous SiO_x layer decreased with increasing substrate temperature as shown in figure 2. Open and closed circles show the top Si and the amorphous SiO_x layers, respectively. It should be noted here that the thicknesses of the top Si and SiO_2 layer, after high-temperature annealing at 1280 °C for 2 h in N_2 atmosphere, were about 67 nm and 27 nm for the implantation at 485 °C, respectively.

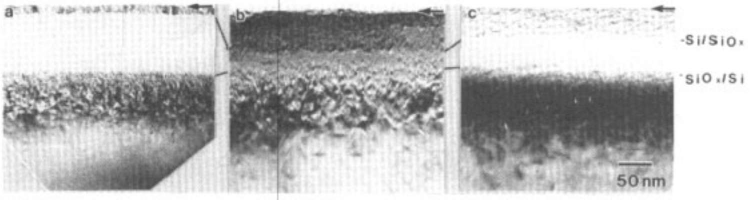

Figure 1. Cross-sectional TEM structure of Si wafers implanted with 25 keV O^+ at (*a*) 280 °C and (*b*) 485 °C with current density 450 $\mu A\ cm^{-2}$, and (*c*) at 485 °C with current density of 10 $\mu A\ cm^{-2}$. O^+ dose was 2×10^{17} ion cm^{-2}. Arrows indicate sample surface.

Si islands appeared in the buried oxide layers in the annealed samples. Crystal orientation of the Si islands in the sample implanted at 485 °C coincided with those of the top Si layer and the Si substrate. This indicates that small crystals remained in the amorphous SiO_x layer during the ion implantation. In the case of 280 °C implanted sample, the Si islands had random crystal orientation. The Si islands are considered to be recrystallized from the amorphous SiO_x state for this low-temperature implantation because of the random crystal orientation. The results obtained here show that the substrate heating resulted in keeping the Si crystal state in the implantation process.

Depth profiles in the O^+ implanted samples measured by the AES analysis before annealing are shown in figure 3. The peak oxygen concentration depth was the same for both samples. The oxygen depth profile for the sample implanted at 485 °C has a narrower half width and a higher peak intensity than the sample implanted at 280 °C. This means that the implanted oxygen gathered more closely around the peak depth under a high substrate temperature. The Si_{KLL} depth profiles were similar for both samples, because the Si_{KLL} intensity is correlated to the total amount of Si. On the other hand, the Si_{LVV} depth profiles, which are sensitive to the bonding state of Si, were found to depend on the implanted temperature. The decrease in the Si_{LVV} intensity at the oxygen peak in high-temperature implanted samples indicates an increase of Si–O bondings.

The observed changes in the implanted oxygen depth profile and the oxygen bonding with silicon are similar to those observed in the high-temperature annealing process. There is no report on this kind of remarkable *in situ* annealing effect in the conventional SIMOX. It can be concluded that the *in situ* annealing effect appeared

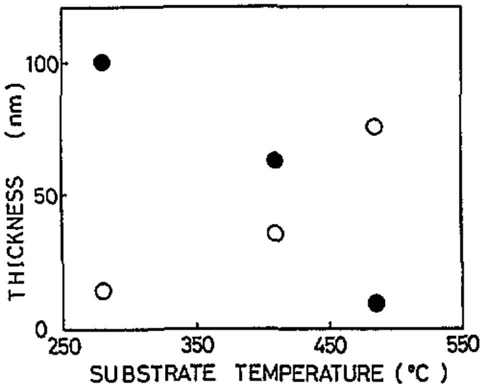

Figure 2. Thicknesses of Si top layer and SiO_x amorphous layer as functions of substrate temperature for as-implanted Si with O^+. Open circles and closed circles indicate Si top layer and amorphous SiO_x layer, respectively.

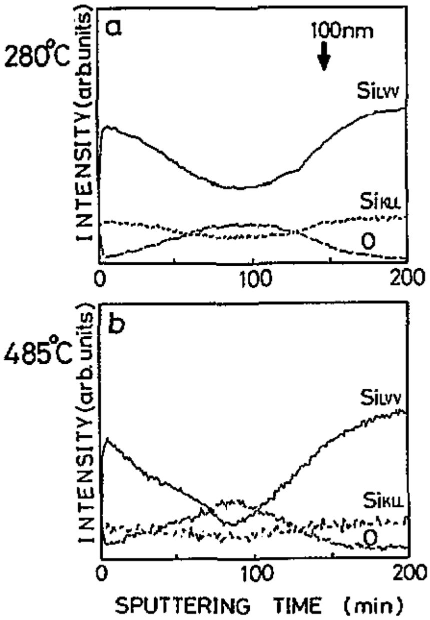

Figure 3. AES signal depth profiles for Si wafers implanted with 25 keV O^+ at (*a*) 280 °C, (*b*) 485 °C. O^+ dose was 2×10^{17} ion cm^{-2} and current density was 450 μA cm^{-2}.

markedly in the low-energy SIMOX because of the low-dose and the narrow oxygen distribution region.

3.1.2. Surface morphology. When the substrate temperature during ion implantation exceeded 535 °C under the same dose (2×10^{17} ion cm^{-2}) and current density (450 μA cm^{-2}), no buried amorphous layer was observed in these specimens without high-temperature annealing by the cross-sectional TEM analysis. The surfaces became uneven at substrate temperature higher than 485 °C. Surface morphology observed by scanning electron microscopy (SEM) is shown in figure 4. A smooth surface was observed in specimens implanted at (*a*) 280 °C and (*b*) 410 °C. Holes were observed for the specimens implanted at (*c*) 485 °C. The shape of the holes was similar to those of the conventional SIMOX [16] although the hole diameter was about twenty times larger than that of the conventional SIMOX. The depth and diameter of the holes were about 20 nm and 500 nm, respectively. However, no cavity structure in the top Si layer was found like those discussed in conventional SIMOX [16, 17]. At temperatures higher than 535 °C (*d*), two different types of hole appeared. One type of hole was similar to the holes appearing in the specimens implanted at 485 °C (*c*). The other type of hole had rounded edges and an almost flat base, and looked like the pore of a pancake or volcanic rock. At temperatures higher than 585 °C (*e*), the second type of hole dominated. The hole size became larger with increasing temperature from 535 °C (*d*) to 710 °C (*f*): the diameter went from 0.15 to 0.9 μm, and the depth from 50 to 250 nm. The size and the density also increased with increasing ion dose.

Total oxygen in the implanted Si, which was estimated by integrating the oxygen signal intensity in the AES depth profile, decreased when the substrate temperature increased over 535 °C, as shown in figure 5. The depth at which the maximum oxygen signal was observed shifted to the surface as shown in figure 6, accompanied by a reduction in the total oxygen content.

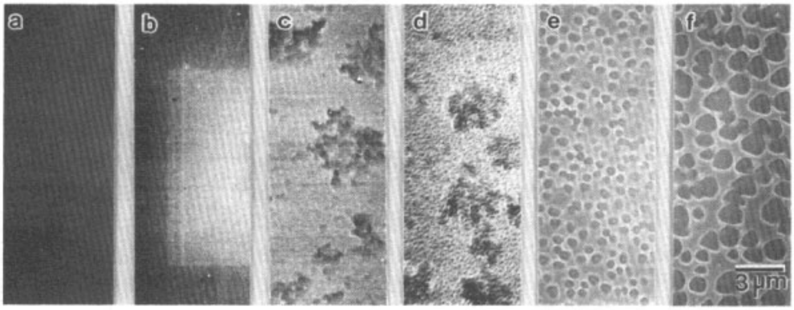

Figure 4. Surface SEM photographs of Si wafers implanted with 25 keV O^+ at (*a*) 280 °C, (*b*) 410 °C, (*c*) 485 °C, (*d*) 535 °C, (*e*) 585 °C and (*f*) 710 °C. O^+ dose was 2×10^{17} ion cm^{-2} and current density was 450 $\mu A\ cm^{-2}$.

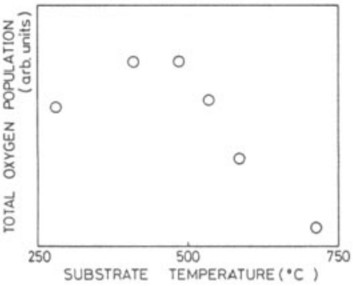

Figure 5. Total oxygen population in O^+-implanted Si estimated from depth profile of AES signal intensity as a function of substrate temperature.

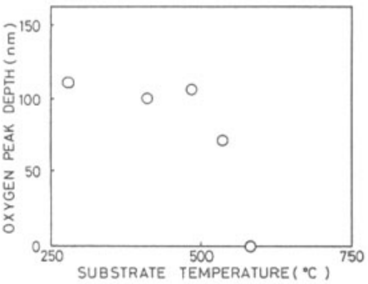

Figure 6. Depth at the maximum oxygen peak in AES depth profiles as a function of substrate temperature for O^+-implanted Si.

It is interpreted that the first kind of hole appearing at lower temperature have little relation to the oxygen release, because both the total oxygen and the oxygen peak depth at 485 °C are almost the same as those at a lower substrate temperature. The holes had no effect on formation of the SOI structure. The surface became flat after annealing at 1280 °C for 2 h. The hole generation mechanism, which may be different from conventional SIMOX, is not understood.

On the other hand, it seems that the second kind of hole appearing at higher temperatures are strongly related to the oxygen release, because the amount of oxygen decreased along with the appearance of the holes. These phenomena can best be interpreted by assuming that SiO sublimation from the surface is a principal process, because it is easier to sublimate SiO in a vacuum at high temperature than Si. High-concentration SiO bonding is formed near the O^+ projection range (80 nm). The projection range coincided with the hole depth observed at 535 °C (*d*). Therefore, the SOI structure cannot be obtained for high substrate temperature (> 535 °C).

It is clear that the substrate temperature range necessary to produce the SOI structure is narrower than that needed for conventional SIMOX. The maximum temperature is limited by the formation of the second type of hole in the low-energy SIMOX process. The minimum temperature is determined by the change of the top Si crystal layer to the amorphous state; oxygen concentration at Si surface is higher than that of conventional SIMOX.

3.2. Dependence on current density

Cross-sectional microstructures for Si implanted with 25 keV O^+ at 485 °C with a dose of 2×10^{17} ion cm^{-2} before high-temperature annealing are shown in figure 1, at different current densities (*b*) 450 $\mu A\ cm^{-2}$ and (*c*) 10 $\mu A\ cm^{-2}$. The substrate temperature increase caused by the ion implantation was about 20 °C and 2 °C for current densities 450 $\mu A\ cm^{-2}$ and 100 $\mu A\ cm^{-2}$, respectively. The temperature changed to (*b*) 505 °C and (c) 485 °C during the ion implantation. SOI structures were formed in both cases. In the sample implanted at 10 $\mu A\ cm^{-2}$, the top Si layer was thinner and the amorphous SiO_x layer was thicker than those implanted at 450 $\mu A\ cm^{-2}$. The interface of the Si layer and the amorphous layer was rather flat at low current density compared with the high-current-density sample. The thicknesses of the top Si and the amorphous SiO_x layers are plotted in figure 7 as a function of current density. Open and closed circles show the top Si and the amorphous SiO_x layer. The thickness of the amorphous SiO_x layer decreased with increasing current density. The thickness of the top Si and SiO_2 layer after annealing at 1280 °C for 2 h were 67 nm and 27 nm at 450 $\mu A\ cm^{-2}$ implantation, respectively. The results showed that the high current density made it easy to retain the crystalline nature of the top Si layer during ion implantation. No evidence of implantation damage increase, which cannot be recovered by high-temperature annealing, was found in the top Si layer even at current densities as high as 450 $\mu A\ cm^{-2}$.

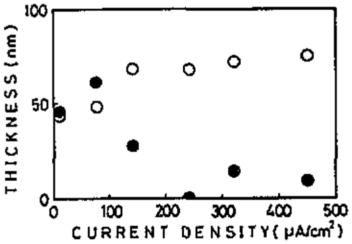

Figure 7. Thicknesses of Si top layer and SiO_x amorphous layer as a function of current density for as-implanted Si with O^+. Open circles and closed circles indicate Si top layer and SiO_x amorphous layer, respectively.

It can be concluded that an increase in current density is equivalent to an increase in the substrate temperature under the implantation condition mentioned above, because the dependence of the layer thickness on the current density measured in the as-implanted samples was similar to its dependence on the substrate temperature.

4. Conclusions

Thin SOI films have been produced by low-energy (25 keV) SIMOX at different substrate temperatures (from 280 °C to about 500 °C) and current densities

(10–450 μA cm^{-2}) with a low oxygen dose of 2×10^{17} ion cm^{-2}. We have observed new effects based on low-energy and low-dose implantation. Heating the substrate to about 485 °C caused marked *in situ* annealing during ion implantation: change in the oxygen depth profile, increase in the number of bonds between Si and O, and keeping the Si crystal state at the surface. Two types of holes appeared in the surface at higher temperature. One type of hole appeared for temperatures higher than 485 °C but did not interfere with SOI structure formation. The other type of hole appeared for temperatures higher than 530 °C, was related to the oxygen release and made it difficult to produce the SOI structure.

The SOI structure was formed by a very high current density of 450 μA cm^{-2} at about 485 °C. The effects of the current density increase were similar to those of the substrate heating. No evidence was observed for serious crystal damage due to the high current density.

It is also important to investigate the effect of the low-energy and the low-dose implantation in relation to implantation conditions and the crystal quality after high-temperature annealing. It will be possible to obtain the SOI substrates with very few defects and dislocations by an appropriate thermal annealing because of the low oxygen dose. Further study is needed on the thermal annealing effects in low-energy SIMOX in order to achieve electrical properties of sufficient quality for device application.

Acknowledgments

The authors would like to thank Y Kubo for continuous encouragement throughout this work. We are much indebted also to K Naganuma and T Sonoda for kindly helping with the AES measurement and giving us useful advice on AES analysis, Y Ikuhara and T Suzuki for helping with TEM observation and for fruitful discussion.

References

[1] Yoshimi M, Wada T, Kato K and Tango H 1987 *Int. Electron Devices Meeting 1987* (New York: IEEE) Technical Digest p 640
[2] Kusunoki S, Yamaguchi Y, Inoue Y, Sugahara K, Miyatake H, Nishimura T and Akasaka Y 1988 *Symp. VLSI Technol. (San Diego, 1988)* (New York: IEEE) Technical Digest p 63
[3] Malhi S D S, Lam H W and Pinizzotto R F 1982 *Int. Electron Devices Meeting 1982* (New York: IEEE) Technical Digest p 107
[4] Yoshimi M, Hazama H, Takahashi M, Kambayashi S, Wada T, Kato K and Tango H 1989 *IEEE Trans. Electron Devices* **ED-36** 493
[5] Colinge J-P 1986 *IEEE Trans. Electron Devices Lett.* **EDL-7** 244
[6] Colinge J-P 1986 *Electron. Lett.* **22** 187
[7] Colinge J-P 1988 *IEEE Electron Devices Lett.* **EDL-9** 97
[8] Sekigawa T and Hayashi Y 1984 *Solid State Electron.* **27** 827
[9] Throngnumchai K, Asada K and Sugano T 1986 *IEEE Trans. Electron Devices* **ED-33** 1005
[10] Yoshimi M, Hazama H, Takahashi M, Kambayashi S and Tango H 1988 *Electron. Lett.* **24** 1078
[11] Hazama H, Yoshimi M, Takahashi M, Kambayashi S and Tango H 1988 *Electron. Lett.* **24** 1266
[12] Wittkower A B and Guerra M A 1989 *Nucl. Instrum. Methods* B **37/38** 512
[13] Ishikawa Y and Shibata N 1991 *Japan. J. Appl. Phys.* **30** 2427
[14] Robinson A K, Marsh C D, Bussmann U, Kilner J A, Li Y, Vanhellemont J, Reeson K J, Hemment P L F and Booker G R 1991 *Nucl. Instrum. Methods* B **55** 555
[15] Namavar F, Cortesi E, Buchanan B and Sioshansi P 1989 *Proc. IEEE SOS/SOI Tech. Conf. (Stateline, NV, 1989)* (New York: IEEE) p 117

[16] Nakashima S and Izumi K 1990 *J. Mater. Res.* 5 1918
[17] Jaussaud C, Stoemenos J, Margail J, Papon A M and Bruel M 1991 *Vacuum* 42 341
[18] Tsuboi H, Hoshino A and Takagi K 1990 *Proc. 13th Symp. ISIAT'90 (Tokyo, 1990)* (Tokyo: IESJ) p 17